The generation of available potential energy by sensible heating: a case study

By ROBERT L. GALL and DONALD R. JOHNSON *Department of Meteorology, University of Wisconsin Madison, Wisconsin 53706*

(Manuscript received May 3, 1971)

ABSTRACT

The importance of the sensible heat transfer from the ocean to the atmosphere within an east coast cyclone is studied using the concept of available potential energy. Both the generation of the storm's available potential energy by this diabatic component and the boundary layer frictional dissipation are estimated. The sensible heat transfer through the interface is calculated by employing the bulk aerodynamic method. The ten meter wind speed is estimated from the surface geostrophic wind models of Rossby & Montgomery (1935) and Lettau (1961). For each model, both a variable wind dependent and a fixed roughness parameter are utilized. The sensible heat flux from the four different computations varied by 50 % showing the sensitivity of the flux estimates to the modeling of the boundary layer winds. From the flux calculations both upper and lower bound estimates of the storm generation by the sensible heating are determined. The upper bound estimate is made by adding all the thermal energy to the superadiabatic surface layer, a few millibars in vertical extent, while the lower bound is determined by distributing the energy uniformly within the dry adiabatic mixing layer extending from a few to several hundred millibars vertically. These bounds reflect the uncertainty in the nature of the energy transfer between the turbulent scale of the boundary layer and the quasi-horizontal scale of the storm. It is postulated that the true generation is bounded by these upper and lower estimates. For the small area of 5.4×10^2 m^2, the lower bound generation estimates range from 0.7 to 1.9 watts m^{-2} at 00z and 1.3 to 3.1 watts m^{-2} at 12z while the upper bound ranges from 1.5 to 3.9 at 00z and 2.6 to 6.1 at 12z for the four different estimates of sensible heat transfer. The boundary layer frictional dissipation increases from 2.7 at 00z to 7.1 watts m^{-2} at 12z. The results indicate that sensible heat generation is significant in the creation of the cyclone's available potential energy, particularly during the early cyclogenetic stage.

1. Introduction

In the wintertime, frequent and intense cyclogenesis occurs along the east coasts of the Asian and North American continents. In these regions large amounts of sensible heat are transferred to the atmosphere when very cold air, originating over the continents, moves eastward over warm oceanic currents. Although this energy transfer is thought to be a major factor in the cyclogenesis, its relative importance to the production of kinetic energy within the storm is an unsolved problem.

Studies of the last decade indicate that the inclusion of sensible heating at the earth's interface is important in predicting storm development. Reed (1958), using a graphical prediction model, found that the addition of this diabatic component in the lower layers of the atmosphere improved forecasts of cyclogenesis in the Gulf of Alaska. Winston (1955) showed that, although horizontal advection of absolute vorticity could partially account for the cyclogenesis in the Gulf of Alaska, substantial errors were present in adiabatic models. Petterssen, Bradbury & Pedersen (1962) found that inclusion of sensible and latent heat transfer from the ocean was necessary to explain the thickness tendency fields in developing storms that formed off the east coast of the United States. Manabe (1958), Pyke (1964), Laevastu (1965), and others showed that sensible heating attained maximum values during and just preceding the rapid cyclogenesis in these regions.

These investigations, however, were not able to answer unequivocally the question of whether the energy that is supplied to the atmosphere from the ocean is an *in situ* energy source for the cyclogenetic process. The total potential energy of the atmosphere (gravitational plus internal) is increased by the heating, but there is no assurance that this process is important in increasing the kinetic energy in the cyclogenetic region. Some insight is provided by noting that the differential heating between the land and ocean causes a strong temperature gradient to develop along the coast. Within the framework of the theory of baroclinic instability (Charney, 1947; Eady, 1949; and others), the increasing horizontal temperature gradient and decreasing static stability by surface heating are important factors in the instability mechanism by which the conversion of potential to kinetic energy is insured.

An alternative approach based on energy principles is to investigate how the inclusion of sensible heating changes the total potential and kinetic energy of the cyclone. However, a diagnostic limitation of this method is that total potential energy changes calculated from data cannot be equated to kinetic energy changes. Errors in the estimates of the time derivatives of the potential energy are of the same order as the actual time derivatives of kinetic energy and equality for the changes of energy is not realized in empirical studies. In order to avoid this problem and others, Lorenz (1955) formulated the theory of available potential energy to explain and study the general circulation. Because the magnitude of available potential energy is closer to that of kinetic energy, errors in the estimates of the temporal derivatives are less than the actual kinetic energy derivatives. Thus the effects of measurement errors are reduced.

The equations that have been primarily used in available potential energy studies were only approximate. Dutton & Johnson (1967) pointed out that for some processes these approximations led to erroneous conclusions. For instance, the approximate expression for the generation of available energy depends on the covariance of heating and the temperature deviation on an isobaric surface. With sensible heating to cold air at the earth's interface, a destruction of available energy is inferred. Dutton & Johnson (1967), however, emphasize that by using the precise expression, which depends on the product of the heating and the deviation of pressure from its average on an isentropic surface, the generation of available energy by sensible heating to cold air will usually be positive.

The equations of both Lorenz (1955) and Dutton & Johnson (1967) were developed for estimating changes of available potential energy of the entire atmosphere. Recently, Johnson (1970) derived the available potential energy of an open system and its rate of change for a limited domain encircling the storm center and extending over the entire vertical extent of the atmosphere. In this study, this framework for the open system is used to estimate the generation of available potential energy by sensible heating for an extratropical cyclone along the east coast. Because the cyclone is the central feature of the open system, the available potential energy and kinetic energy of the open system as well as their rate of change will be identified with those of the storm. The boundary layer frictional dissipation is also estimated in order to compare the energy source by sensible heating with the energy sink.

List of symbols

A	available potential energy of the storm volume
π	total potential energy of the storm volume
p	pressure
T	temperature
ϱ	density
θ	potential temperature
θ_T	potential temperature at the top of the atmosphere
V_θ	volume of the region encircling the storm and extending from the earth's surface to the top of the atmosphere
J	Jacobian of the transformation from Cartesian to isentropic coordinates
ε	efficiency factor
Q_m	rate of heat addition per unit mass
F	sensible heat flux
F_s	upward sensible heat flux from the ocean
U_g	surface geostrophic wind speed

$U_a(z)$ wind speed at anemometer height z
$\theta_a(z)$ potential temperature of the air at anemometer height z
$\theta_s(o)$ sea surface potential temperature
$C_a(z)$ aerodynamic drag coefficient at anemometer height z
C_g geostropic drag coefficient
k von Karman's constant
z_0 surface roughness parameter
α angle between the geostrophic wind vector and the surface shear stress
0 dissipation of kinetic energy
p_t pressure at top of the mixing layer
c_p specific heat at constant pressure
c_v specific heat at constant volume
R_d gas constant for dry air
$\varkappa$ R_d/c_p
g gravity
f Coriolis parameter
r subscript to denote variable of the reference atmosphere

2. Energy equations for the available potential energy of a storm

A. *The definition*

The available potential energy after the definition of Margules (1903) is

$$A = \pi - \pi_r \tag{1}$$

where π is the total potential energy of a region encircling the storm and π_r is the total potential energy of the same region after an adiabatic redistribution to a hydrostatically stable horizontal stratification (called the reference state) in the absence of lateral boundary work and advection. From Johnson (1970), the time rate of change of the available potential energy of a volume surrounding the storm in symbolic form is

$$\frac{dA}{dt} = -C(A,K) + B(A) + W(A) + G(A) \tag{2}$$

where $C(A, K)$ is the conversion of the available potential energy to kinetic energy, $B(A)$ is the relative advection of energy into the storm's moving volume, $W(A)$ is the change of available potential energy from boundary work and $G(A)$ is the generation of available energy within the storm volume. The expression for the generation is

$$G = \int_{V_\theta} (1 - (p_r/p)^\varkappa)\, \varrho J Q_m \, dV_\theta \tag{3}$$

where the reference pressure defined by the mass distribution in the actual atmosphere is

$$p_r = g \int_\theta^{\theta_T} \overline{\varrho J}\, d\theta \tag{4}$$

The overbar denotes a horizontal average over that portion of the potential temperature surface contained in the limited region. Without any approximations an alternate generation expression is

$$G = \int_m \varepsilon\, Q_m \, dm \tag{5}$$

where m is the total mass of the open system and the efficiency factor is defined to be

$$\varepsilon = (1 - (p_r/p)^\varkappa) \tag{6}$$

The physical basis for the efficiency factor lies in the definition of the available potential energy of the open system. Normally, heating or cooling changes the total potential energy of both the natural and the reference atmospheres differently. The efficiency factor provides the weighting of the heating field to determine this difference, i.e., the generation of available potential energy. Heating (cooling) at pressures higher and cooling (heating) at pressures lower than the isentropic mean will result in generation (destruction) of the storm's available potential energy.

3. Sensible Heating

In theory, the generation of available potential energy expressed by (3) is valid for all scales of the continuum including those with hydrostatic imbalances and statics instabiities (Dutton & Johnson, 1967). In application, however, the data density, the necessary employment of the hydrostatic assumption, and the approximate model of sensible heating preclude any claim for precision. Attention will be focused on assumptions which may invalidate conclusions, while approximations that may introduce 20 to 30% estimation errors are accepted as inevitable. The goal is to establish from the viewpoint of available potential energy whether sensible heating is an important process in the frequent cyclogenesis of these oceanic regions and not the precise magnitude of the generation which undoubtedly varies with each synoptic event.

The form of the generation shows that the diagnostics may be separated into two distinct aspects—the efficiency distribution and the sensible heat addition. The efficiency distribution, which is determined by the quasi-hydrostatic large scale structure of the storm, is presented later. The modeling of the sensible heat addition is presented in this section.

A. *Sensible heat flux*

For the turbulent sensible heat flux within the time and space scale of the cyclone, the ocean behaves as a strong and continuous heat source in comparison with energy added to the boundary layer over continental regions. Thus, only the sensible heat flux through the ocean's interface need be considered.

Fig. 1 portrays a schematic showing three layers of the boundary region: the surface layer, the adiabatic layer, and the free troposphere. The surface layer, at most a few millibars in depth, is characterized by superadiabatic lapse rates. The adiabatic or mixing layer with its constant potential temperature extends from a few to several hundred millibars in depth. Ideally, the top of the mixing layer is the lowest level for which the vertical sensible heat flux becomes negligible in comparison with its surface value. Deardorf (1966) emphasized that significant sensible heat flux in stable air only occurs if the lapse rate is nearly adiabatic. Consequently, the top of the mixing layer should coincide with the level where the stability increases. In general the top of the mixing layer does not coincide with the level for which the wind approaches geostrophic balance, i.e., the upper level normally defined for the planetary boundary layer.

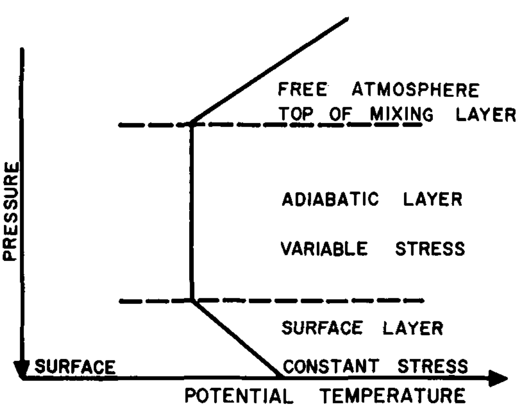

Fig. 1. Schematic distribution of potential temperature through the boundary layer.

A practical method for estimating the sensible heat flux is the bulk aerodynamic method given by

$$F_s = c_p\, C_a(z)\, [\theta_s(0) - \theta_a(z)] U_a(z) \qquad (7)$$

Its utility and limitations are thoroughly discussed in several excellent summaries (e.g. Deacon & Webb, 1962; Roll, 1965). The choice of a height for the air temperature and wind speed is not extremely critical since the drag coefficient, $C_a(z)$, is adjusted for the appropriate height. In this study a commonly selected height of 10 m is used.

The use of air temperature ordinarily observed from a ship's bridge height of less than 10 m (from 6 to 9 m, Roll (1965)) will produce a conservative estimate of the sea-air temperature difference for the model. Within the surface layer of constant stress where the upward sensible heat flux is large, potential temperature decreases rapidly with height. See the schematic distribution in Fig. 1. An air temperature measurement taken in the region of six to nine meters produces an underestimate of the idealized 10 m temperature difference and thus also the sensible heat flux.

In the derivation of the bulk aerodynamic method it is assumed that the sensible heat transfer coefficient is equal to the momentum transfer coefficient, i.e., the drag coefficient, in a neutral atmospheric surface layer (Deacon & Webb, 1962). Observational results for neutral conditions indicate that the functional dependence of the drag coefficient is of the form

$$C_a(10\text{ m}) = (a + bU_a\,(10\text{ m}))10^{-4};$$
$$1 \leqslant U_a \leqslant 20\text{m/sec} \quad (8)$$

Sheppard (1958) suggests that the empirical constants a and b are 0.8 and 1.14 while Deacon & Webb (1962) suggest 11.0 and 0.7. However, Manier's (1962) empirical result that a is 7.9 and b is 0.96 from a least squares fit to the data of 9 different investigators was utilized primarily because of his interest in the heat balance for the North Atlantic region (Manier & Möller, 1961). For the same region, Petterssen, Bradbury & Pedersen (1962) set a equal to 26.0 and b equal to zero. In this study, the maximum 10 m wind speed was 27 m sec^{-1} while the predominate speeds were 12 m sec^{-1}. As a result, the magnitudes of the transfer coefficients were usually 10 to 12% less than the values suggested by Sheppard (1958) and Deacon & Webb (1962), and approximately equal to Petterssen et al. (1962). From (7), the flux estimates are similarly conservative by the same proportionality since the sensible heat transfer is directly proportional to the transfer coefficient's magnitude.

No attempt is made to incorporate the dependence of the sensible heat transfer coefficient upon bulk stability because of the limited vertical resolution of synoptic data. Garstang's (1967) analysis for low latitude sensible heat transfer within synoptic scale systems indicates that the effective transfer coefficient is double the neutral coefficient for the large negative lower limit of his bulk Richardson number equal to -0.325. Deardorff's (1968) recent theoretical analysis of the ratio of the diabatic transfer coefficient to its neutral value also provides support for an argument that the estimated transfer coefficients based on neutral theory are only 50 to 75% of their effective values in the regions of extreme free convection. Thus these factors indicate that the sensible heat flux estimates of this study will tend to be conservative.

In the bulk aerodynamic calculations, the ten meter wind speed was estimated from the surface geostrophic wind field by two methods, one from the model proposed by Rossby & Montgomery (1935), the other by Lettau (1961). In Rossby & Montgomery's formulation, hereafter called Model 1, the wind speed for the constant stress layer is

$$U_a(z) = 3/2[(0{,}065\ U_g)k \sin \alpha \ln ((z + z_0)/z_0)] \quad (9)$$

where α is the angle between the geostrophic wind vector and the surface shear stress. In this study a constant α of 20° was used. In Lettau's (1961) formulation, hereafter denoted Model II, the wind speed for the constant stress layer is

$$U_a(z) = U_g(C_g/k) \ln ((z + z_0)/z_0) \quad (10)$$

where C_g, the geostrophic drag coefficient from Kung's (1963) empirical regression relation, is

$$C_g = 4.01[\ln (U_g/z_0 f) - 1.865]^{-1} \quad (11)$$

At this point the only undetermined parameter is the surface roughness. Over the land, a constant value of 100 cm was assumed. Over the ocean, the state of the sea, i.e., its roughness, depends strongly on the wind speed. Empirical data indicate that z_0 varies from 10^{-4} cm for light winds to 50 cm for winds in excess of 30 m/sec. For the oceanic regions, two calculations were made for each model, one with a constant z_0, the other with a variable z_0. For the constant z_0 calculations. a value of 1 cm was selected as it applies to moderate wind speeds of 10–15 m sec^{-1}. For the variable z_0 calculations, the surface roughness over the ocean was determined from the approximate relation for adiabatic theory (Manier, 1962; Roll, 1965) that

$$z_0 / \simeq 10^3 e^{-k/\sqrt{C_D}} \quad (12)$$

A first guess of one-half the geostrophic wind was used for the 10 m wind speed to estimate the drag coefficient by (8), then from (12) and either (10) or (11), the 10 m wind estimate was revised using this estimate of the drag coefficient. Three such iterations were sufficient to achieve a stable estimate for the 10 m wind speed.

B. *Vertical distribution of sensible heat addition*

After the sensible heat enters the atmosphere through the earth-air interface, it diffuses vertically. If this vertical transfer within the atmosphere were solely by molecular conduction and the motion were quasi-hydrostatic, this transfer would be confined to the surface layer. The generation equation (5) could be applied directly because the efficiency factor is essentially constant within this layer. However, the extreme heating of this layer produces large hydrostatic instabilities and free convection. This in combination with the mechanically forced tubulence within the boundary layer results in a continued upward vertical transfer of sensible heat throughout the boundary layer. The theoretical aspects of this scalewise heat transfer have been discussed by Priestley (1967).

From the aspect of the generation of available potential energy, distribution of all the thermal energy throughout the surface layer is justified if the frictional dissipation of the vertical kinetic energy in the boundary layer is negligible or small. A portion of the available potential energy generated within the surface layer manifests itself through hydrostatic instability as the vertical kinetic energy of free convection. If this convective kinetic energy is adiabatically converted back into potential energy by the negative buoyancy forces, an entropy conserving processs, the entire amount of available potential energy generated within the surface layer must be realized at the hydrostatic synoptic scale. However, if the convective kinetic energy is frictionally dissipated into thermal energy, a local entropy increasing process that serves to diffuse the thermal energy within the mixed layer, not all the available potential energy generated can be realized at the synoptic scale.

Because the exact nature of the energy exchange between the micro-, meso- and macroscales is not known, the generation estimates are computed for two distributions of heating. One generation estimate representing the upper bound is computed by confining the thermal energy to the surface layer; a lower bound is computed by assuming that the heat addition per unit mass is uniform within the mixing layer. For horizontal homogeneity and the hydrostatic approximation, the heat addition per unit mass is

$$Q_m = g\,\partial F/\partial p \qquad (14)$$

where F is the turbulent heat flux. Thus for constant flux divergence, Q_m is independent of pressure. This distribution, possibly the most realistic, is consistent with the view that the turbulent redistribution serves to diffuse the internal energy and maintain the condition of $\theta \neq \theta(p)$ in the mixing layer. For a uniform translating mixing layer, the substantial derivative $d\theta/dt$ must remain independent of pressure, implying that Q_m is a constant except for its pressure dependency with $d\theta/dt$. However, this dependency remains slight due to the restricted vertical extent of the mixing layer with respect to pressure.

4. The case study

In February 1968, an intense upper tropospheric vortex existed over Eastern Canada for a duration of several weeks. In the lower troposphere a series of polar outbreaks occurred with cold air flowing southward from Canada over the Gulf Stream. South of Newfoundland several cyclones developed rapidly in the lower troposphere along the poleward boundary of the Gulf Stream. The strong sea surface temperature gradient in this region is shown in the North Atlantic portion of a hemispheric analysis obtained from the Naval Fleet Weather Central of Monterey (Fig. 2). Of these cyclones, the storm that formed on February 14, 1968 intensified at a rate much faster than is usually

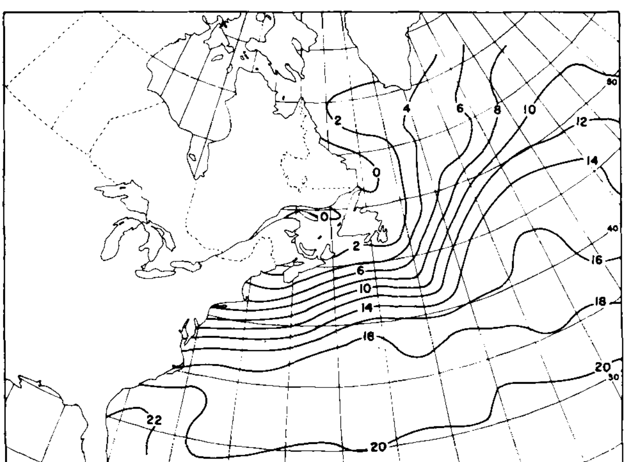

Fig. 2. Sea surface temperature (°C) for the North Atlantic Ocean, February 14, 1968.

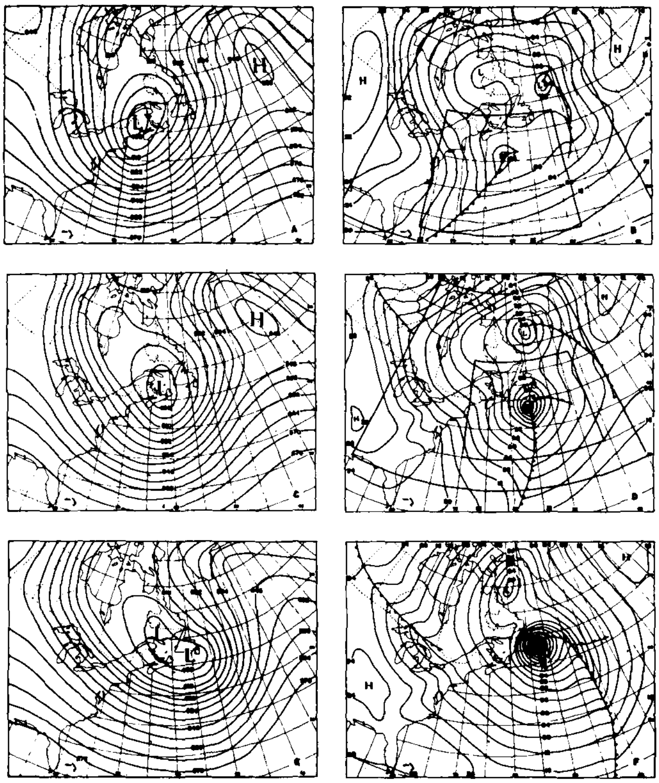

Fig. 3. The 500 mb height analysis (geopotential decameters) and surface analysis (millibars) for 0000Z, February 14, (A and B), 1200Z, February 14, (C and D), and 0000Z February 15, (E and F), 1968. The dashed rectangles in B and D delineate the large and small regions used to compute the generation of storm available potential energy.

observed, and since the sensible heat flux from the ocean to the atmosphere was extremely large, this storm was selected for this study.

A. *The synoptic description*

In Figs. 3*a* through *f* the surface and 500 mb analyses portray the sequence of synoptic events for the 24 hour period from 0000Z on the 14th through 0000Z on the 15th of February. On February 13 at 0000Z (not shown) the upper tropospheric vortex was centered just northwest of Maine. A short wave with a strong vorticity maximum was embedded in the vortex just north of Lake Huron. Within the next 14 hours, the center of the vortex moved slowly southeast to the position over Maine shown in Fig. 3*b*, while the vorticity maximum moved counterclockwise about the vortex to a position southeast of the vortex center. In the low troposphere, the short wave was accompanied by a surge of cold air whose leading edge at 1800Z, February 13 (not shown) was marked at the surface by a weak trough extending south-southwestward along the east coast of the United States. For the succeeding six hours, this trough advanced rapidly eastward and reinforced the cold front lying well off shore that was associated with the previous cold outbreak.

At 0000Z on the 14th and at a point just in advance of the 500 mb short wave trough the first evidence of cyclogenesis appeared along the old cold front about 100 nautical miles south of Sable Island (see Fig. 3*a*.) Ships in the vicinity reported pressure falls of 6 mb in three hours. The low's central pressure decreased at a rate of almost 2 mb per hour throughout the following 24 hours. By 1200Z (Figs. 3*c* and *d*) the center was located 200 nautical miles south of Newfoundland, the central pressure had reached 967 mb and winds near the center exceeded 50 knots. The surface low attained its greatest intensity shortly after 0000Z February 15. The pressure and wind profiles for St. Johns, Newfoundland in Fig. 4*b* attest to the remarkable intensity of this storm.

In the ESSA composite picture for February 14 shown in Fig. 5 the cyclone already appears

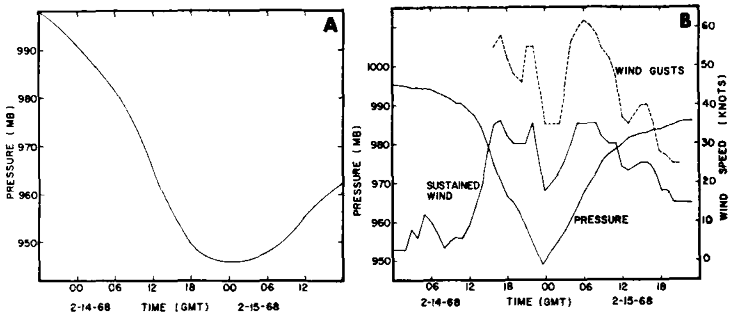

Fig. 4. The central pressure of the east coast cyclone of February 14–15, 1968 (A) and the pressure and wind speed at St. Johns, Newfoundland during its passage (B).

to be strongly occluded. The time of the picture corresponds to local noon which is midway between synoptic time of Fig. 3*c* and *e*.

For the diagnostic computations the synoptic times 0000Z and 1200Z, February 14, were selected. Fig. 4*a* shows that the earlier time is near the beginning of cyclogenesis while the latter time is in the period of the most rapid storm development.

B. *The analysis*

The existence of a dry adiabatic lapse rate in the mixing layer means that potential temperature is no longer a single-valued function of height and the isentropic representation fails. Constant height or pressure analysis must be utilized in this layer. Above the mixing layer the isentropic portrayal of atmospheric structure no longer fails. The depth of the mixing layer must be known for matching of the two representations.

Above the mixing layer isentropic pressure analyses for every five degrees from 250° to 320° were prepared. The potential temperature distribution of the mixing layer was specified by surface analyses of potential temperature. For the specification of the upper pressure of the mixing layer, approximate soundings were constructed for the oceanic regions from the istentropic analysis of the stable troposphere.

Fig. 5. Composite mosaic of satellite pictures from ESSA 3 for the North Atlantic Ocean for February 14, 1968.

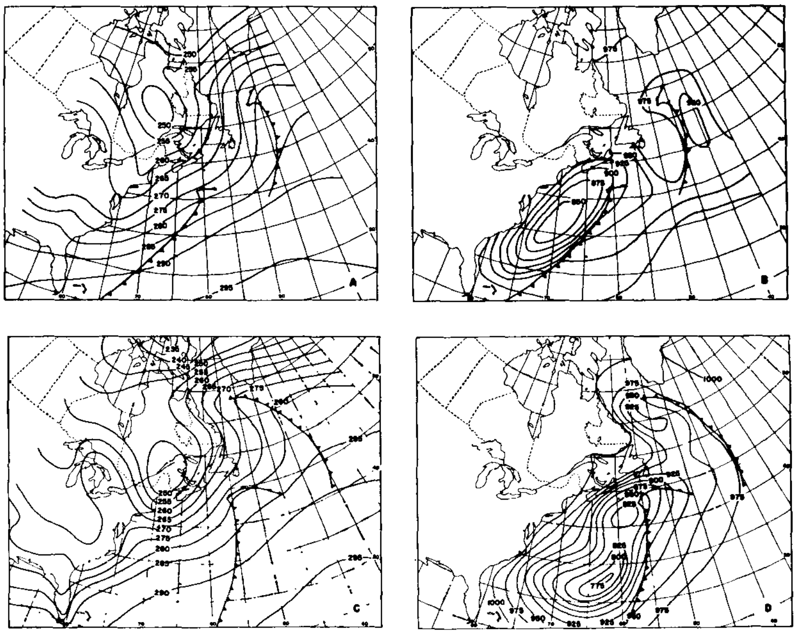

Fig. 6. Surface potential temperature (°K) distribution (A and C) and the pressure (mb) of the top of the mixing layer (B and D). Upper figures: 0000Z; lower figures: 1200Z, February 14, 1968.

The lapse rate of the lowest stable portion of these soundings was extended downward until it intersected the dry adiabat of the surface potential temperature. The intersection defined the upper pressure of the mixing layer.

This interpolation–extrapolation technique was first conducted for regions in close proximity to actual data and was extended laterally to sparse data regions. The pressure distribution of the upper boundary of the mixing layer that is presented in Figs. 6*b* and *d* shows that its depth sometimes exceeds 200 mb. When these analyses are combined with the surface pressure (Figs. 3*a* and *c*) and potential temperature analysis (Figs. 6*a* and *c*) the mass-potential temperature distribution of the mixing layer is specified. Although this procedure is approximate, it is probably the best possible with the limited data.

C. *The isentropic topography*

Only six isentropic surfaces are presented in Figs. 7*a* through *f* to protray the three dimensional structure. The most strikting feature at 1200Z on the 14th is the extremely cold air which appears as a mound from the earth's surface to the stratosphere. Near the surface, the center of the cold air is located northwest of Maine. Its axis tilts southeastward with height to a position just east of Maine on the 295°K surface. On the 275°K and 285°K surfaces, a ridge of cold air extends from the main center of cold air southeastward toward the surface pressure center located south of Newfoundland. The isentropic surfaces along this ridge slope from relatively high levels over the cold air, and descend steeply towards the ocean with the 275°K and 285°K surfaces becoming vertical in the mixing layer. The very steep gradient of pressure is evidence of the vortex's strong baroclinic zone associated with the short wave jet core that was important in initiating cyclogenesis.

Over the Great Lakes modification due to sensible heating is evident on the 265°K surface (Fig. 7*b*). The intersection of this surface with the ground partially circumscribes this region because the water is warmer than 265°K. To the west and south, the cold air has subsided and spread laterally into a thin sheet to cover most of the eastern United States.

D. *The efficiency factor analysis*

The efficiency factor distribution on an isentropic surface is determined solely by the

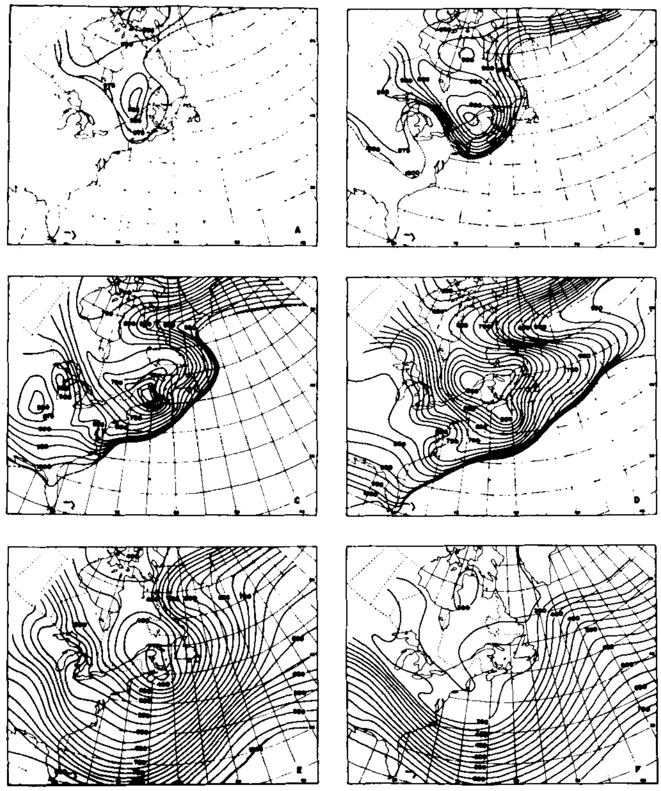

Fig. 7. Pressure analysis on the isentropic surfaces 255°K(A), 265°K(B), 275°K(C), 285°K(D), 295°K(E), and 305°K(F) for 1200Z, February 14, 1968.

pressure because the reference pressure is a single-valued function of the potential temperature. This is still true for adiabatic regions since even there the original definition, that the reference atmosphere is realized by preserving the mass-potential temperature distribution, is utilized. The analytics of available energy in atmospheres with local static instabilities is presented in Section 2.6 of Dutton & Johnson (1967).

For computational purposes the reference pressure after (4) is

$$p_r(\theta_k) = \frac{\sum_{j=1}^{N} \sum_{j=1}^{m} p_{ij}(\theta_k) Aij}{\sum_{i=1}^{N} \sum_{j=1}^{M} A_{ij}} \tag{15}$$

where θ_k is the kth isentropic surface, p_{ij} is the pressure at the ijth grid point of the $N \times M$ latitude–longitude grid, and A_{ij} is the area of the grid mesh at the ijth point. The grid interval was two degrees. The restriction that the surface air potential temperature at a grid point is not equal to the potential temperature of a kth isentropic surface is used. On the underground portion of the isentropic surface, the surface pressure is assigned (Lorenz, 1955).

Fig. 8 presents the 12Z reference pressure profiles for the small and large regions delineated in Fig. 3. The large area includes the 500 mb vortex; the small area includes the extratropical cyclone of the lower troposphere. The similarity of the profiles is evidence that the selection of the lateral extent of the volume is not a critical factor in this study.

Two cross sections of the efficiency distribution for 12Z, February 14 are presented to illustrate the regions where diabatic heating is important. The first cross section, Fig. 9a, is orientated north–south along 56° W transects

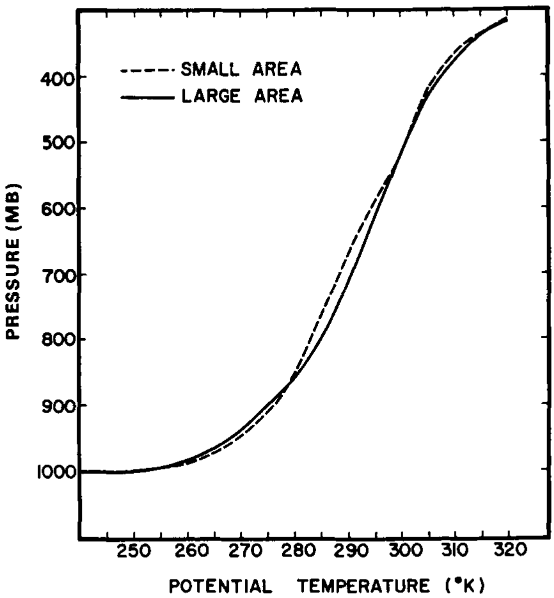

Fig. 8. Reference pressure distribution for the large and small areas.

the atmosphere just west of the storm and parallels the cold front. The second cross section, Fig. 9*b* runs east–west through a point just south of the storm center.

The efficiency pattern is similar to Hahn & Horn's (1969) distribution for maturing cyclones. A nearly vertical zero efficiency isopleth exists in the middle troposphere. Southeast of the storm center, the efficiencies are positive up to relatively high altitudes, with a maximum near 700 mb. In the vicinity of the baroclinic zone, the zero line assumes an "S" shape with a positive region extending over the negative region of the colder air.

The 00Z and 12Z surface analyses presented in Figs. 10*a* and *c* show that efficiencies are positive with one exception. In eastern Canada the cold air and lower-than-average surface pressures combine to give a limited region of small negative values. Along the east coast of the U.S., the efficiencies were small. The large positive efficiencies encountered in the southern Atlantic illustrate that for a given amount of sensible heating, the generation is largest when the energy is added to warmer air. Still, the maximum sensible heating occurs further

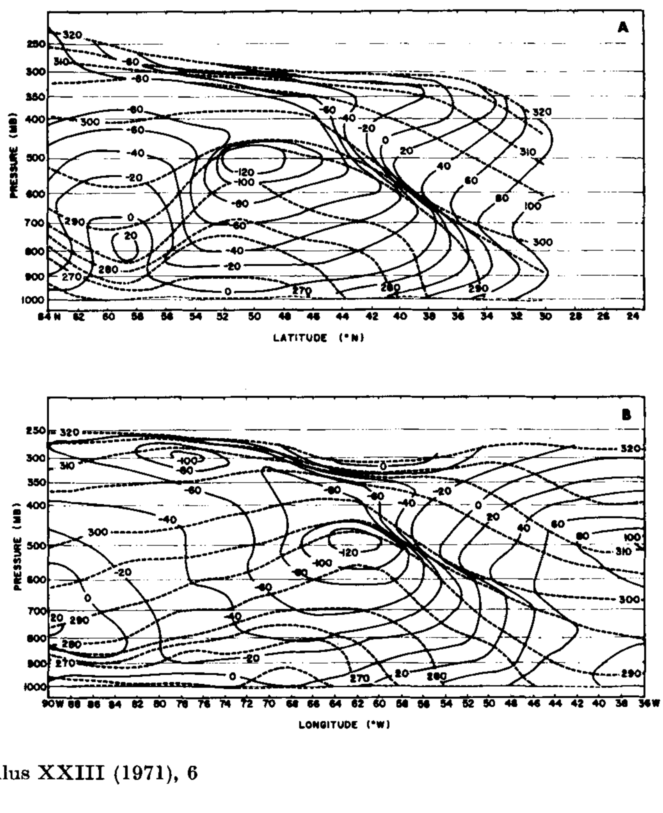

Fig. 9. Cross-sections orientated north–south along 56°W longitude (A) and east–west along 24° N latitude (B), 1200Z, February 14, 1968. Solid and dashed isopleths are efficiency factor ($\times 10^{-3}$) and potential temperature (°K) respectively.

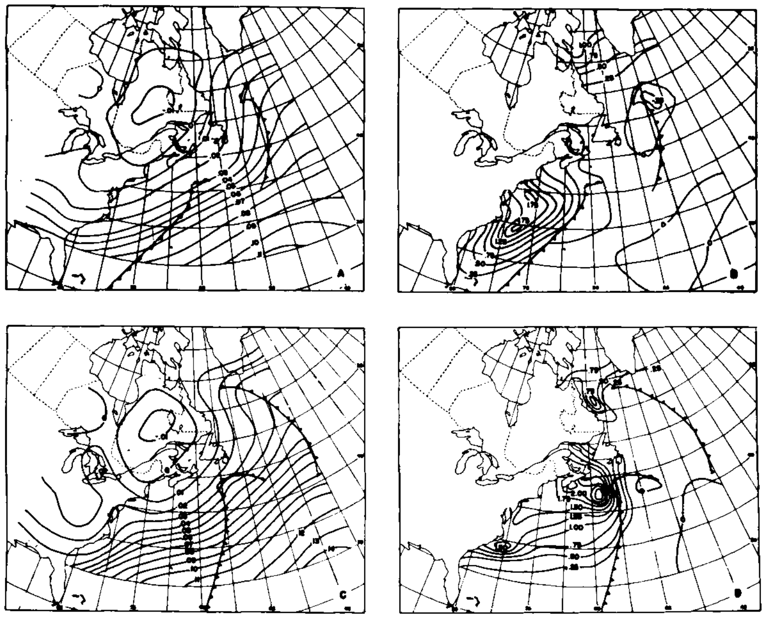

Fig. 10. Surface efficiency factors for the large area (A and C) and sensible heat flux (cal cm^{-2} sec^{-1} $\times$ 10^{-2}) from the ocean (B and D). Upper figures: 0000Z; lower figures: 1200Z, February 14, 1968.

north in colder air and regions of reduced efficiencies. Thus, maximum generation occurs where the turbulent transfer of energy is large and the efficiency is still significantly positive.

E. *The sensible heat flux*

The surface sensible heat fluxes determined from the bulk aerodynamic method and Model I with z_0 variable are presented in Figs. 10*b* and *d*. Positive upward flux exists over the entire low pressure area. Even ahead of the cold front the flux to the relatively cold polar air from previous outbreaks is still positive. At 00Z, the greatest upward flux occurs along the U.S. coast. As the system develops, the area of maximum values translates with the storm center and a secondary maximum moves southward along the U.S. coast.

Exceptions to upward sensible heat flux occur approximately 1 000 km in advance of the cold front (Figs. 10*b* and *d*), and at 00Z in a region surrounding the northern cyclone. The modified polar air in these regions is caught in the return circulation of the developing vortex. In general, downward flux extrema are an order of magnitude less than upward flux maxima.

In the computations of the 10 m wind speed, estimates by Models I and II differed by 2 m per sec in areas of light geostrophic winds and by 4 m per sec for winds of 10–15 m per sec. In a comparison of predicted and reported ship winds Model I with z_0 variable consistently produced the best results in this study.

In the aerodynamic method with a variable drag coefficient, the dependence between sensible heat flux and wind speed is quadratic. Thus the differences between Model I and II wind speed predictions is amplified in estimating sensible heat flux. In Tables 1 and 2 the average heat transfer predicted by Model I with z_0 variable is at least twice that of Model II with z_0 fixed. The variations of the maximum flux in Table 3 are similar. The results illustrate the sensitivity of flux estimates to differences in modeling.

In a comparison of maximum fluxes (Table 4), our results compare favorably with Petterssen's et. al. (1962) and Manabe's (1958) estimates. The difference between our estimate of 25.8 $\times$ 10^{-3} cal cm^{-2} sec^{-1} and Petterssen's et. al. estimate of 16.7 cal cm^{-2} sec^{-1} is due to the quadratic dependence on wind speed in this study in contrast to the linear dependence utilized by Petterssen's et. al. (1962). At a 10

Table 1. *Average sensible heat flux (cal cm^{-2} sec^{-1} $\times 10^{-3}$) for large area—14 February, 1968*

Hour of observation	0000Z		1200Z	
Model ...	I	II	I	II
Variable z_0	1.5	0.8	2.6	1.5
Constant z_0	0.9	0.6	1.7	1.1

Table 2. *Average sensible heat flux (cal cm^{-2} sec^{-1} $\times 10^{-3}$) for small area—14 February, 1968*

Hour of observation	0000Z		1200Z	
Model ...	I	II	I	II
Variable z_0	2.9	1.6	5.0	2.8
Constant z_0	1.8	1.2	3.5	2.1

m wind speed of 18 m sec^{-1} and an equal sea-air temperature difference, the flux predicted in both studies is nearly equal.

Manabe's estimate of 11.9×10^{-3} cal cm^{-2} sec^{-1} is the maximum average sensible heat flux during a cold outbreak computed for a budget volume encompassing the entire Sea of Japan. Very likely the heating along the Siberian and Korean coasts just as the coldest air commences its over-water trajectory exceeded the average value by a factor of two or three. Pyke's (1964) estimate of 2.5×10^{-3} cal cm^{-2} sec^{-1} for weather ship P in the Gulf of Alaska during a period of strong northerly flow is for a region far south of the maximum heating over the Japanese current.

F. *The generation*

In the discussion of the vertical distribution of sensible heating it was argued that generation for the synoptic scale should be some intermediate value between upper and lower bounds. The maximum generation for the large and small areas (Tables 5 and 6) is from Model I with z_0 variable. In the large area upper bound estimates are 1.9 watts m^{-2} at 00Z and 2.8 watts m^{-2} at 12Z and the lower bound estimates are 1.0 and 1.6 watts m^{-2} respectively. The minimum lower bound estimates from Model II with z_0 constant are 0.4 watts m^{-2} at 00Z and 10.6 watts m^{-2} at 12Z. The variation between lower and upper bound estimates is only slightly larger than the variation between the various model estimates. Thus the uncertainty of the generation due to our lack of knowledge of the vertical exchange of energy is compounded by the uncertainty in the modeling of sensible heat flux.

The estimates for the small area (Table 6) are roughly double the estimates for the larger area (Table 5), and indicate the concentration of the diabatic effects within the storm circulation. At 12Z all the estimates for the small area are significantly positive. If the wind model with the most realistic predictions (Model I—z_0 variable) provides the most realistic sensible heat flux estimates, then the generation should be within the range of 1.9 and 3.9 watts m^{-2} for 00Z and 3.1 and 6.1 watts m^{-2} for 12Z.

The results of a test to determine if the depth of the mixing layer critically affects the computed generation are presented in Table 7. In this test the generation was estimated by assigning a uniform pressure of 900 mb for the top of the mixing layer. The comparison of the test and former results shows that in the large area generation estimates with a constant p_t are slightly lower. For the small area, this result is reversed. The use of a constant p_t of 900 mb in the small area effectively lowers the top of the mixing layer with the result that the energy is added at higher pressures.

Table 3. *Maximum sensible heat flux (cal cm^{-2} sec^{-1} $\times 10^{-3}$)—14 February, 1968*

Hour of observation ...	0000Z		1200Z	
Model ...	I	II	I	II
Variable z_0	18.5	10.2	25.8	15.1
Constant z_0	12.0	7.6	23.4	13.0

Table 4. *Maximum sensible heat flux (cal cm^{-2} sec^{-1} $\times 10^{-3}$) found by other investigators*

Investigator	Sensible heat flux
Petterssen et al. (1962)	16.7
Pyke (1964)	2.5
Manabe (1958)	11.9
Gall & Johnson (1970)	25.8

Table 5. *Average generation (watts m^{-2}) for the large area with a variable mixing layer depth*

Upper and lower bounds are from uniform heating of the surface and mixing layers, respectively

Time of observation ...	00Z		12Z	
Model ...	I	II	I	II
Upper bound				
Variable z_0	1.9	1.0	2.8	1.5
Constant z_0	1.1	0.7	1.8	1.2
Lower bound				
Variable z_0	1.0	0.6	1.6	0.9
Constant z_0	0.6	0.4	1.0	0.6

Table 6. *Average generation (watts m^{-2}) for the small area with a variable mixing layer depth*

Time of observation ...	00Z		12Z	
Model ...	I	II	I	II
Upper bound				
Variable z_0	3.9	2.1	6.1	3.4
Constant z_0	2.4	1.5	4.2	2.6
Lower bound				
Variable z_0	1.9	1.0	3.1	1.7
Constant z_0	1.1	0.7	2.0	1.3

Table 7. *Average generation (watts m^{-2}) with the top of the mixing layer assumed to be 900 mb*

Variable z_0 was used in both models

Time of observation ...	00Z		12Z	
Model ...	I	II	I	II
Large area	0.9	0.5	1.2	0.7
Small area	1.9	1.0	3.2	

The spatial distribution of the generation estimates from uniform heating within the surface and mixing layers are presented in Figs. 11*a* throgh *d*. While these patterns are for the large volume, they are nearly identical to distributions based on the small volume because of their similar reference pressure distributions. An important feature when the energy is added to the surface layer is that nearly all the estimates are positive since the reference pressure is almost always less than the pressure of the top of the surface layer. In constrast, when the heat is added to the mixing layer there is a region of negative values west of the storm center (Fig. 11*d*). Here the

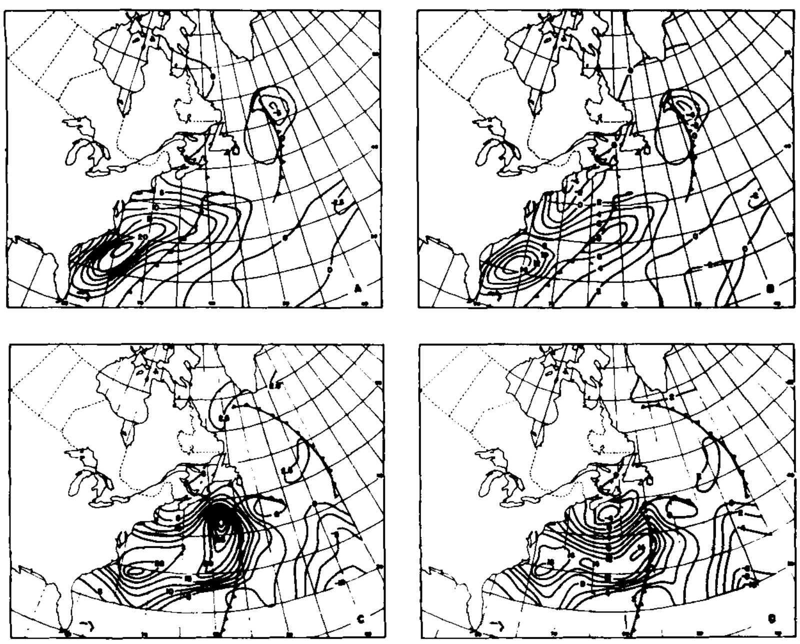

Fig. 11. Distribution of generation (watts m^{-2}) within the large area for uniform heating of the surface layer (A and C) and the mixing layer (B and D). Upper figures: 0000Z; lower figures: 1200Z, February 14, 1968.

Table 8. *Comparison between the approximate and exact generations estimates (watts m^{-2}) by sensible heating for 12Z, February 14, 1968*

Area	Large	Small
Approximate	−1.1	−7.6
Exact/upper bound	2.8	6.1
Exact/lower bound	1.6	3.1

reference pressure is greater than the mean pressure of the mixing layer, thus, the local generation becomes negative. Further from the dome of cold air, the reference pressure decreases until it is less than the mean pressure of the mixing layer and the generation becomes positive. This factor causes the maximum generation in Figs. 11*b* and *d* to be displaced further southward than the corresponding maximum in Figs. 11*a* and *c*.

If the approximate generation expression (Lorenz, 1955) which depends on the covariance of the isobaric temperature and heating deviation is utilized, the estimates, shown in Table 8, are negative. The standard atmosphere's static stability of γ equal to 6.5°C/km was used in these computations. Negative estimates such as these have led to the conclusion that sensible heating destroys eddy available potential energy by reducing the temperature contrast between air masses. Thus, the role of sensible heating in eddy generation has been erroneously interpreted by some investigators.

G. *The comparison of dissipation and generation*

The frictional dissipation of kinetic energy in the boundary layer was estimated using Lettau's (1961) formulation given by

$$D = \varrho C_g^2 \, U_g^3 \cos \alpha$$

The departure angle between the geostrophic wind vector and the surface shear stress, α, was assumed to be 20°.

Table 9 presents the frictional dissipation using the land ocean distribution of the roughness parameter from Model I, variable z_0. Generation estimates are included for comparison. The results show that the storm generation by sensible heating constitutes a significant fraction of the frictional dissipation. At 00Z the average frictional dissipation for the large area exceeds the upper bound generation estimate. For the small area, the lower bound estimate is approximately equal to the dissipation while the upper bound is nearly double the dissipation. By 12Z the dissipation exceeds the upper bound estimate by the sensible heat component. The results indicate that *in situ* generation by sensible heating is important in maintaning the kinetic energy of the storm against frictional dissipation. In the relative sense, the generation by sensible heating is more important for the smaller intense storm scale than for the larger scale.

In the bulk aerodynamic computations the enhancement of sensible heat transfer in the super adiabatic surface layer was disregarded by not including a drag coefficient dependence on the bulk Richardson number. Thus, the upper and lower generation bounds are very likely conservative. Just how important the sensible heating is can only be determined with more precise modeling.

The spatial distribution of the frictional dissipation is presented in Figs. 12*a* and *b*. The most striking feature is the large dissipation of 70 watts/m² associated with the maximum winds located just to the rear of the vortex center (Fig. 12*b*). This is higher than the dissipation reported by Petterssen et al. (1962). Their values for a composite cyclone which are effectively averages did not exceed 40 watts/m². However, because dissipation is proportional to the cube of the surface geostrophic wind, the wind speed associated with 70 watts/m² need be only slightly greater than one corresponding to 40 watts/m².

Elsewhere the dissipation did not exceed 10 watts/m² except near the Northern storm and over land. The higher dissipation overland

Table 9. *Boundary layer frictional dissipation and generation estimates (watts m^{-2}) from Model I, variable z_0*

Time of observation ...	00Z		12Z	
Area ...	Large	Small	Large	Small
Dissipation	2.1	2.2	4.7	7.1
Generation bounds				
Upper	1.9	3.9	2.8	6.1
Lower	1.0	1.9	1.6	3.1

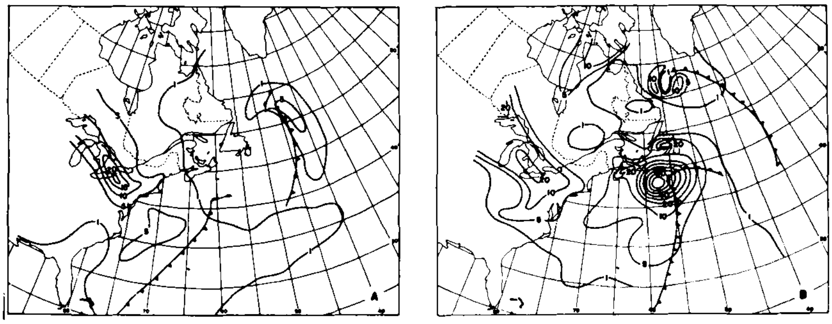

Fig. 12. Frictional dissipation of kinetic energy (watts m^{-2}) in the boundary layer for 0000Z (A) and 1200Z (B), February 14, 1968.

is due to the greater roughness. Kung's (1963) average zonal values for the Northern American continent indicate that the value for z_0 of 100 cm over land is possibly too large and that the dissipation may be overestimated.

In Table 10 total sensible heat flux, generation and frictional dissipation are summarized. The generation appears to remain relatively constant during the cyclogenetic period. This behavior is accounted for by two offsetting factors. Figs. 10*a* and *c* show that efficiency factors along the coast decrease with time as the center of the cold air mass moves toward the coast, a factor leading to decreased generation. During the same period sensible heating increases and tends to increase the generation. Eventually the translation of the polar air over the ocean will lead to its modification and the sensible heating and generation will decrease. Thus, the effect of sensible heating must be more important early in the storm's development than in later stages.

Table 10. *Total sensible heat flux, dissipation, and generation estimates (10^{13} watts) by Model I with variable z_0*

Large and small areas are 1.67×10^{13} and 0.54×10^{13} m^2

Time of observation ...	00Z		12Z	
Area ...	Large	Small	Large	Small
Sensible heat flux	124.0	79.0	184.0	113.0
Dissipation	4.0	1.4	7.6	3.8
Generation bounds				
Upper	3.6	2.5	4.7	3.3
Lower	2.0	1.2	2.7	1.7

6. Remarks and conclusions

Although precise estimates of the generation by sensible heating cannot be stated from this study, the condition that sensible heat flux generates a significant amount of available potential energy during cyclone development is established. Evidence is provided that energy added to the atmosphere by molecular transfer across the earth's interface is actually a direct energy source to the quasi-horizontal scales of atmospheric motion. The extended horizontal domain of the molecular process primarily determined by large scale conditions was undoubtedly an important element in the forcing of the large scale cyclogenesis.

Estimation of generation is crucially dependent on the nature of the turbulent exchange of energy within the boundary layer. The upper bound estimates given by confining the thermal energy within the surface layer are nearly twice the lower bound estimates given by distributing the heating throughout the mixing layer. From the thermodynamic viewpoint and the exact energy equations, the upper bound estimate would be true if the buoyant mass element retained its identity and entropy in seeking its equilibrium level. Thus its turbulent vertical kinetic energy would be transformed back into available potential energy of the synoptic scale by negative buoyancy. However, because the mass element loses its identity through diffusion within the boundary layer the entropy must increase and the generation of available potential energy at the synoptic scale will tend toward the lower bound estimate.

From the upper and lower bounds estimated in this study, the computations indicate that the *in situ* generation by sensible heating is somewhere between 34 to 177 % of the boundary layer frictional dissipation during the cyclogenic stage and from 18 to 86 % during the mature stage

Some importance for other diabatic processes in development may be inferred from Bullock & Johnson's (1971) results for the mature stage of a mid-latitude cyclone. For an area of 0.62×10^{13} m^2 over the continental US, Bulllock & Johnson found that the storm generation by latent heating and infrared emission was 7.0×10^{13} watts and 0.7×10^{13} watts, respectively, a total of 7.7×10^{13} watts. If these estimates are adjusted to the small area of this study and added to the generation by sensible heating at 12Z, the total generation would be 8.5×10^{13} watts for the lower bound and 10.1×10^{13} watts for the upper bound. Both estimates exceed the boundary layer frictional dissipation by at least a factor of two. These results provide support for the hypothesis that the *in situ* generation within the storm scale is sufficient to offset its frictional dissipation in the formative and mature stages, and is important in the development process.

A complete theory for cyclogenesis along the east coast or for that matter anywhere, awaits a better understanding of the thermodynamic and mechanical interaction between all scales of the motion. The solution will involve mass, angular momentum as well as energy. It is undoubtedly the interaction of several processes that result in the complex sequence of events we call cyclogenesis.

Acknowledgements

The authors wish to thank Professor Lyle Horn for his helpful suggestions, Mr Daniel Dolson for his assistance in data preparation and Miss Sharon Nicholson and Mr Si Chung Ok for drafting.

The research was jointly supported by the National Environmental Satellite Center, Environmental Science Services Administration, ESSA E-8-69(G) and the Atmospheric Sciences Section, National Science Foundation, NSF Grant GA-10997. Partial support was provided by the National Aeronautics and Space Administration through a fellowship and the Wisconsin Alumni Research Foundation and the National Science Foundation in the form of a grant for computational funds and the use of computer facilities.

REFERENCES

Bullock, B. R. & Johnson, D. R. 1971. The generation of available potential energy by latent heat release in a mid-latitude cyclone. *Mon. Wea. Rev. 99*, No. 1, 1–14.

Charney, J. G. 1947. The dynamics of long waves in a baroclinic current. *Journ. of Met. 4*, 135–162.

Deacon, E. L. & Webb, E. K. 1962. Interchange properties between the sea and air. *The sea*, vol. 1 (ed. M. N. Hill), pp. 43–87. Wiley, New York.

Deardorf, J. W. 1966. The counter gradient heat flux in the lower atmosphere and in the laboratory. *Journ. of the Atm. Sci. 23*, 503–506.

Deardorf, J. W. 1968. Dependence of air–sea transfer coefficients on bulk stability. *Journ. of Geophys. Res. 73*, 2549–2557.

Dutton, J. A. & Johnson, D. R. 1967. The theory of available potential energy and a variational approach to atmospheric energetics. *Advances in Geophysics*, vol. 12, 333–436. Academic Press, New York.

Eady, E. T. 1949. Long waves and cyclone waves. *Tellus 1*, 33–52.

Garstang, M. 1967. Sensible and latent heat exchange in synoptic scale systems. *Tellus 19*, 492–508.

Hahn, D. G. & Horn, L. H. 1969. The generation of available potential energy in a mid-latitude cyclone. Final Rept. ESSA Grant WBG 52, Dept. of Meteorology, University of Wisconsin, Madison.

Johnson, D. R. 1970. The available potential energy of storms. *Journ. of the Atm. Sci. 27*, 727–741.

Kung. E. C. 1963. Climatology of aerodynamic roughness parameter in the planetary boundary layer over the northern hemisphere. Annual Report, Contract DA-36-039-AMC-00878, Department of Meteorology, University of Wisconsin.

Laevastu, L. 1965. Synoptic scale heat exchange and its relations to weather. *Proceedings of the Air–Sea Interaction Conference, Tallahassee, Fla., 1965*, Tech. note 9-SAIL-1.

Lettau, H. H. 1961. Theoretical wind spirals in the boundary layer of a barotropic atmosphere. Annual Report, Contract DA-36-039-80282, Department of Meteorology, University of Wisconsin, Madison.

Lorenz, E. N., 1955: Available potential energy and the maintenance of the general circulation. *Tellus 7*, 157–167.

Manier, G. 1962. Zur Berechnung der latenten und fühlbaren Wärmeströme von der Meeresoberfläche an die Luft. *Geofisica Pura e Applicata* (Milan) *52*, 189–213.

Manier, G. & Möller, F. 1961. Determination of heat balance at the boundary layer over the sea. Final Report, Contract AF 61(052)-315, Meteoro-

logisch-Geophysikalisches Institut, Johannes Gutenberg-Universität, Mainz, Germany.
Manabe, S. 1958. On the estimation of energy exchange between the Japan Sea and the atmosphere during the winter based upon the energy budget of both the atmosphere and the sea. *Journ. Met. Soc. Japan 36*, 123–133.
Margules, M. 1903. Über die Energie der Stürme. *Jahr. Kais. Zent. für Meteor., Vienna.* In a collection of translations by Cleveland Abbe, 1910, "The Mechanics of the Earth's Atmosphere", 3rd collection, *Smithsonian Misc. Coll.*, vol. 51, no. 4, 1910.
Petterssen, S., Bradbury, D. L. & Pedersen, K. 1962. The Norwegian cyclone models in relation to heat and cold sources. *Geophys. Publik. 24*, 243–280.
Priestley, C. H. B. 1967. Handover in scale of the fluxes of momentum, heat etc., in the atmospheric boundary layer. In *Boundary Layer and Turbulence, The Physics of Fluids Supplement 1967*, 38–46.
Pyke, C. B. 1964. On the roll of air–sea interaction in the development of cyclones. *Bull. Amer. Met. Soc. 46*, 4–15.
Reed, R. J. 1958. A graphical prediction model incorporating a form of non-adiabatic heating. *Journ. of Met. 15*, 1–8.
Roll, H. U. 1965. *Physics of the marine atmosphere.* Academic Press, New York.
Rossby, C. G. & Montgomery, R. B. 1935. The layer of frictional influence in wind and ocean currents. *Papers in Physical Oceanography and Meteorology*, Massachusetts Institute of Technology and Woods Hole Oceanographic Institute, vol. 3, no. 3.
Sheppard, P. A. 1958. Transfer across the earth's surface and through the air above. *Quart. Journ. Royal Met. Soc. 84*, 205–224.
Winston, J. S. 1965. Physical aspects of rapid cyclogenesis in the Gulf of Alaska. *Tellus 7*, 481–500.

ОБРАЗОВАНИЕ ДОСТУПНОЙ ПОТЕНЦИАЛЬНОЙ ЭНЕРГИИ ВСЛЕДСТВИЕ НАГРЕВАНИЯ

Изучается перенос тепла от океана к атмосфере в циклонах восточного побережья с использованием концепции доступной потенциальной энергии. Оценивается образование доступной потенциальной энергии в циклонах как путем нагревания, так и вследствие диссипации из-за трения в пограничном слое. Перенос тепла через поверхность раздела вычисляется с помощью аэродинамического метода. Из модели Россби и Монтгомери (1935) и Леттау (1961) геострофического ветра у поверхности следует оценка скорости ветра 10 м/сек. Для каждой модели используются как постоянный параметр шероховатости, так и переменный, зависящий от ветра. Поток тепла по четырем различным вычислениям меняется в пределах 50 %, демонстрируя чувствительность оценок потока к моделированию ветра в пограничном слое. По вычислениям потока находятся оценки верхней и нижней границы образования циклона вследствие нагревания. Верхняя оценка получается из условия, что вся тепловая энергия уходит в сверхадиабатический поверхностный слой вертикальной протяженностью в несколько миллибаров, тогда как нижняя граница получается путем распределения энергии равномерно внутри сухоадиабатического слоя перемешивания, простирающегося от нескольких до нескольких сотен миллибар по вертикали. Эти пределы отражают неопределенность природы переноса энергии от турбулентного масштаба пограничного слоя к квазигоризонтальному масштабу циклона. Постулируется, что фактическое образование энергии заключено между верхней и нижней оценками. Для малой области $5,4 \times 10^2$ м^2 нижняя оценка меняется от 0,7 до 1,9 ватт м$^{-2}$ в полночь и от 1,3 до 3,1 ватт м$^{-2}$ в полдень, тогда как верхняя граница меняется от 1,5 до 3,9 в полночь и от 2,6 до 6,1 в полдень для четырех различных оценок переноса тепла. Диссипация из-за трения в пограничном слое возрастает от 2,7 в полночь до 7,1 ватт м$^{-2}$ в полдень. Результаты показывают, что приток тепла играет важную роль в образовании доступной потенциальной энергии циклона, особенно на ранней стадии циклогенеза.